

第12回若手科学者によるプラズマ研究会
2009年3月17日 原子力機構那珂核融合研究所 ITER会議棟

トロイダルプラズマ・基礎直線プラズマにおける乱流の非線形過程の実験的研究

永島芳彦、山田幸太郎
東大新領域

本研究は、九州大学伊藤研究室の特別推進研究(16002005)を中心に、東京大学、日本原子力研究開発機構、核融合科学研究所、間の共同研究で実施され、また科学研究費補助金(18760637)の援助を受けて遂行されました。



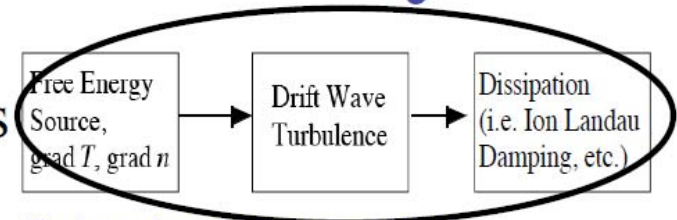
Importance of bispectrum [1,2] in Lagrangian nonlinearity

For example: Meso-scale structures driven by **turbulence Reynolds stress** (e.g. drift wave-zonal flow systems)

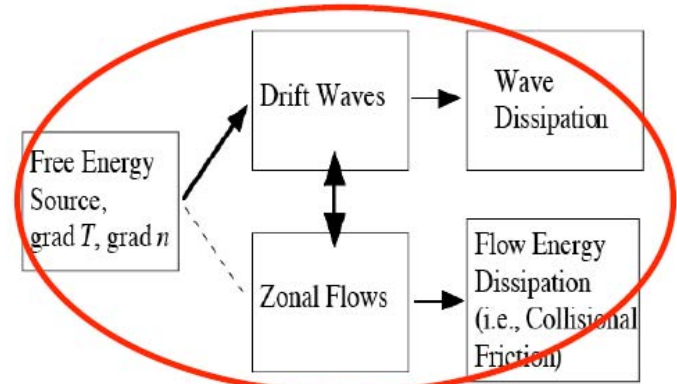
Energy transfer equation

$$\frac{\partial}{\partial t} |\bar{v}_\theta|^2 + 2\bar{v}_\theta^* \frac{\partial}{\partial r} \langle \tilde{v}_r \tilde{v}_\theta \rangle = -\mu |\bar{v}_\theta|^2$$

bispectral functions.



Classic paradigm of drift wave turbulence



New paradigm of drift wave-zonal flow turbulence

Figure 1. New paradigm for the plasma turbulence.
Quoted from P.H. Diamond, et al., PPCF 47 R35 (2005)

- [1] M. Hino, *Spectral Analysis* (Asakura Shoten, Tokyo, 1977).
- [2] Y. Kim and E. Powers, *IEEE Trans. Plasma Sci.* **PS-7**, 120 (1979).

Bispectral functions

Bispectrum, spectrum of third order correlation function

$$B(\omega_1, \omega_2) = \int_{-\infty}^{\infty} \int_{-\infty}^{\infty} d\tau_1 d\tau_2 \overline{x(t)y(t+\tau_1)z(t+\tau_2)} e^{i(\omega_1\tau_1 + \omega_2\tau_2)}$$
$$= \left\langle X(\omega_1)Y(\omega_2)Z^*(\omega_1 + \omega_2) \right\rangle,$$

squared bicoherence

$$\hat{b}^2(\omega_1, \omega_2) = \frac{\left| \left\langle X(\omega_1)Y(\omega_2)Z^*(\omega_1 + \omega_2) \right\rangle \right|^2}{\left\langle |X(\omega_1)Y(\omega_2)|^2 \right\rangle \left\langle |Z(\omega_1 + \omega_2)|^2 \right\rangle},$$

total bicoherence

$$\sum_{\omega_1 + \omega_2 = \text{const}} \hat{b}^2(\omega_1, \omega_2),$$

biphase

$$\Theta = \tan^{-1} \left(\frac{\text{Im}(\hat{B}(\omega_1, \omega_2))}{\text{Re}(\hat{B}(\omega_1, \omega_2))} \right)$$

[1] M. Hino, *Spectral Analysis* (Asakura Shoten, Tokyo, 1977).

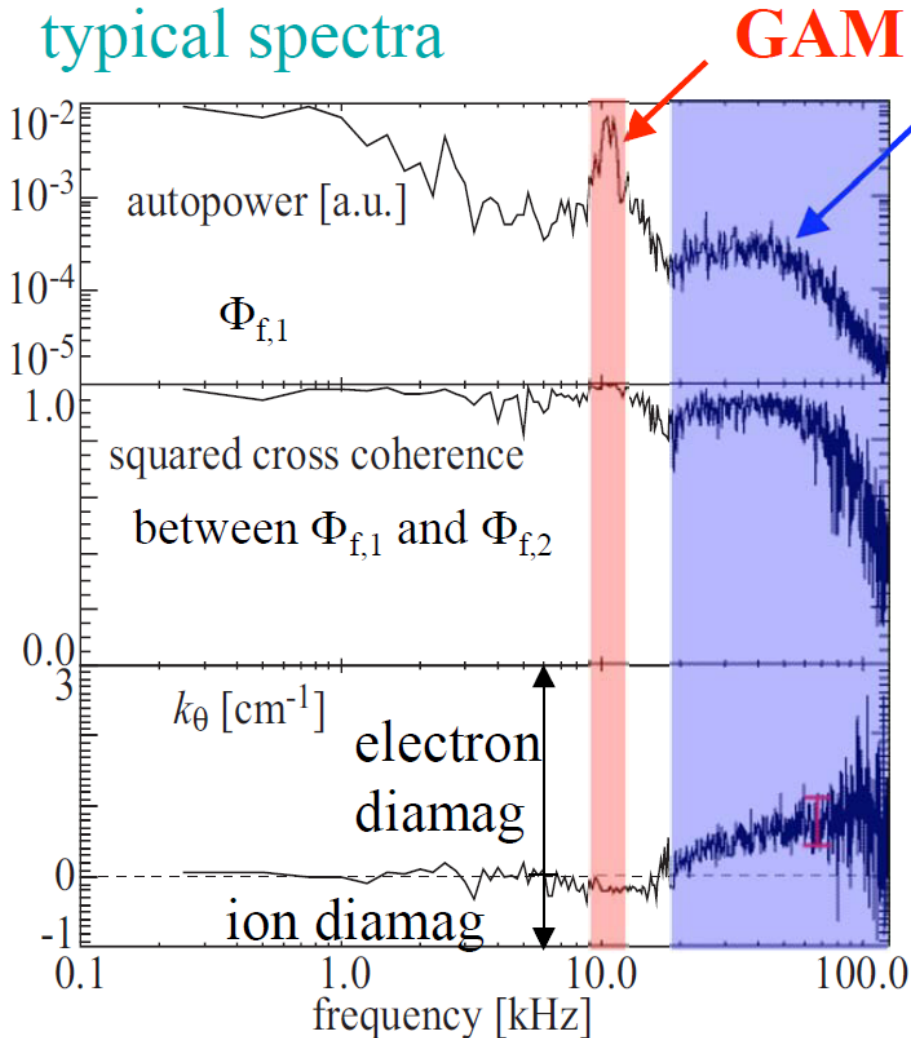
[2] Y. Kim and E. Powers, *IEEE Trans. Plasma Sci.* **PS-7**, 120 (1979).

Results of JFT-2M edge plasma

Relationship between geodesic acoustic mode (GAM) and turbulence

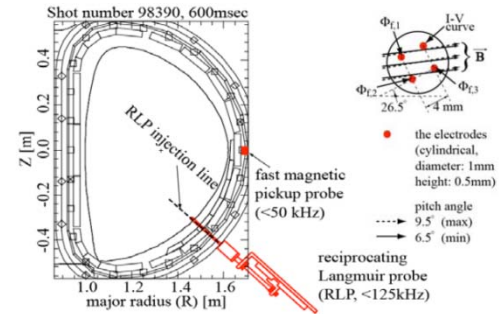
Experimental apparatus on JFT-2M and geodesic acoustic mode

typical spectra

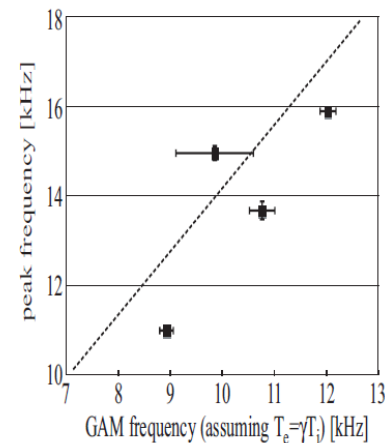


GAM

Broad-band Turbulence (drift waves)

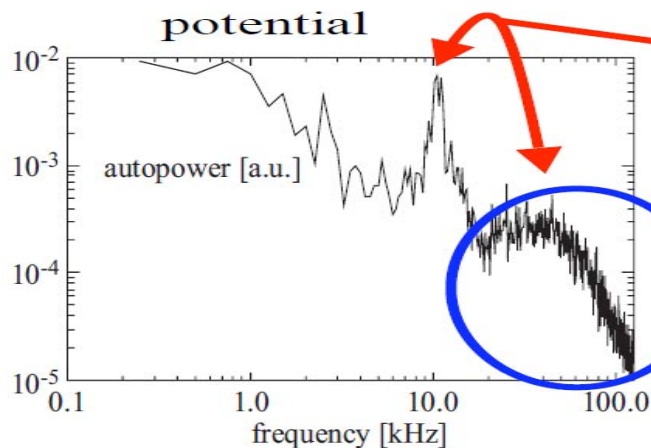


GAM frequency and spectral peak frequency

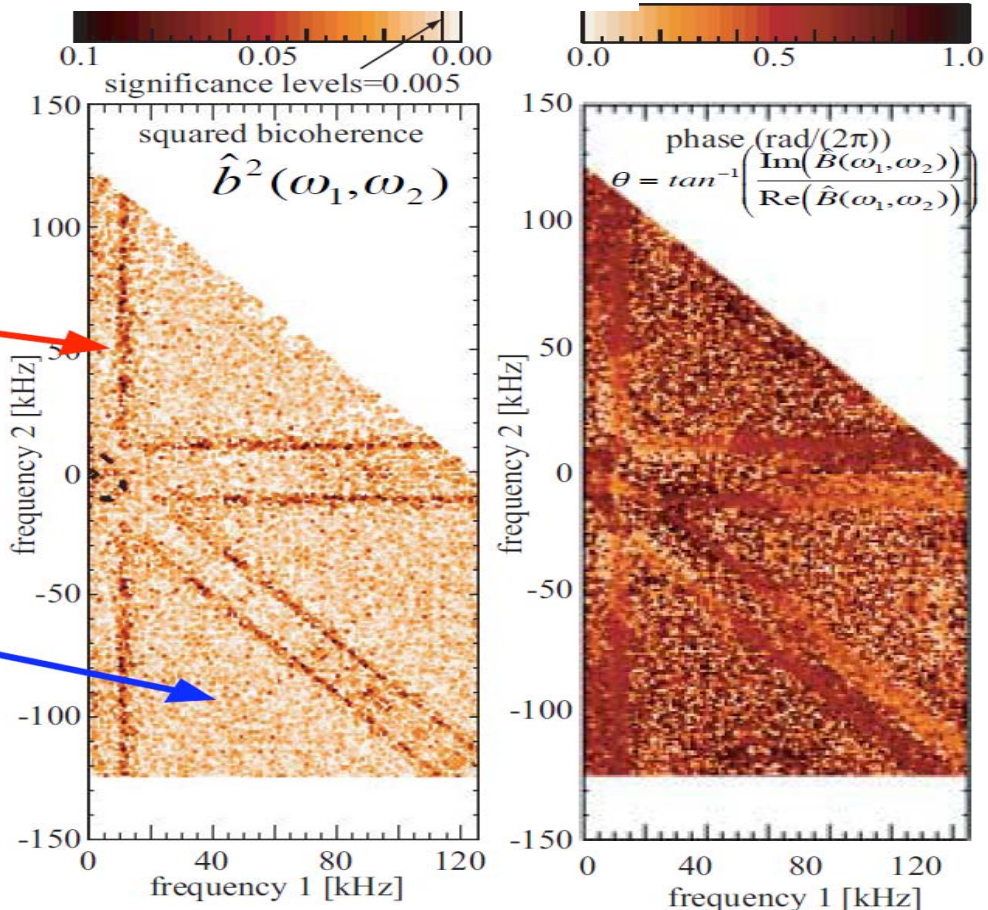


Results of bicoherence and biphase planes

Nonlinear coupling between GAM and turbulence



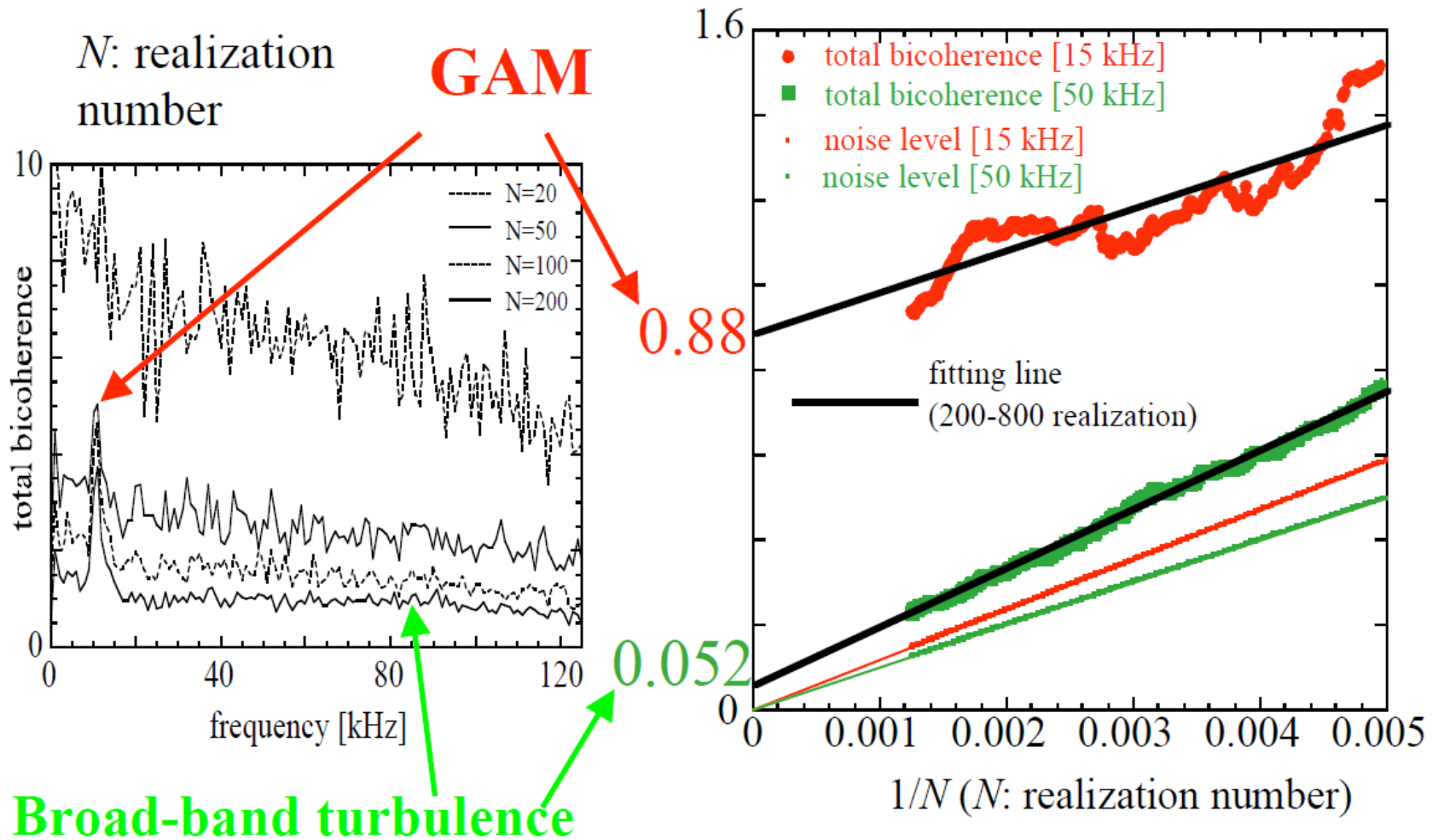
Nonlinear coupling among turbulence



GAM is nonlinearly coupled to the broad-band fluctuations.

The biphase is constant around $\sim \pi$ in the nonlinear coupling between GAM and turbulence.

Convergence property of total bicoherence



Comparison with theoretical prediction

Experimental parameters measured by the RLP and the HIBP are,

M : frequency segments

ρ_s : ion Larmour radius at T_e

k_θ : drift wave poloidal wavenumber

q_x : zonal flow radial wavenumber

$k_\perp = \sqrt{k_\theta^2 + k_x^2}$

$h(k_\perp \rho_s)$: normalized turbulence deccorelation rate

τ : deccorelation time

ω_* : drift frequency

ϕ_z : zonal flow potential amplitude

ϕ_d : drift wave potential amplitude

$$M = 125, \rho_s = 0.2 \text{ cm}, k_\theta \sim 1.5 \text{ cm}^{-1}$$

$$q_x \sim 0.5 \text{ cm}^{-1}, k_\perp \sim \sqrt{2}k_\theta,$$

$$h(k_\perp \rho_s) = \tau^{-1} \omega_*^{-1} \phi^{-1} \sim 0.4,$$

$$\tau \sim 6 \text{ } \mu\text{sec evaluated by autocorrelation time,}$$

$$\omega_* \sim 4 \times 10^5 \text{ rad/sec, and } \phi_z^2 / \phi_d^2 \sim 1.0$$

$$\sum \hat{b}^2(\omega) \sim 4M \left(\frac{1}{h(k_\perp \rho_s)} \frac{q_x k_\perp^2 \rho_s^3}{1 + k_\perp^2 \rho_s^2} \right)^2 \frac{\phi_z^2}{\phi_d^2} + 3 \left(\frac{1}{h(k_\perp \rho_s)} \frac{k_x k_\perp^2 \rho_s^3}{1 + k_\perp^2 \rho_s^2} \right)^2$$

The estimated total bicoherence from theory at **GAM of ~0.9** and **the ambient fluctuations of ~0.05** are similar to the converged bicoherence.

Total bicoherence dependence of GAM amplitude

Comparison with theory^[6]:

$$\sum \hat{b}^2(\omega) \sim 4M \left(\frac{1}{h(k_{\perp} \rho_s)} \frac{q_s k_{\perp}^2 \rho_s^3}{1 + k_{\perp}^2 \rho_s^2} \right)^2 \left(\frac{\phi_z^2}{\phi_d^2} \right) + 3 \left(\frac{1}{h(k_{\perp} \rho_s)} \frac{k_s k_{\perp}^2 \rho_s^3}{1 + k_{\perp}^2 \rho_s^2} \right)^2$$

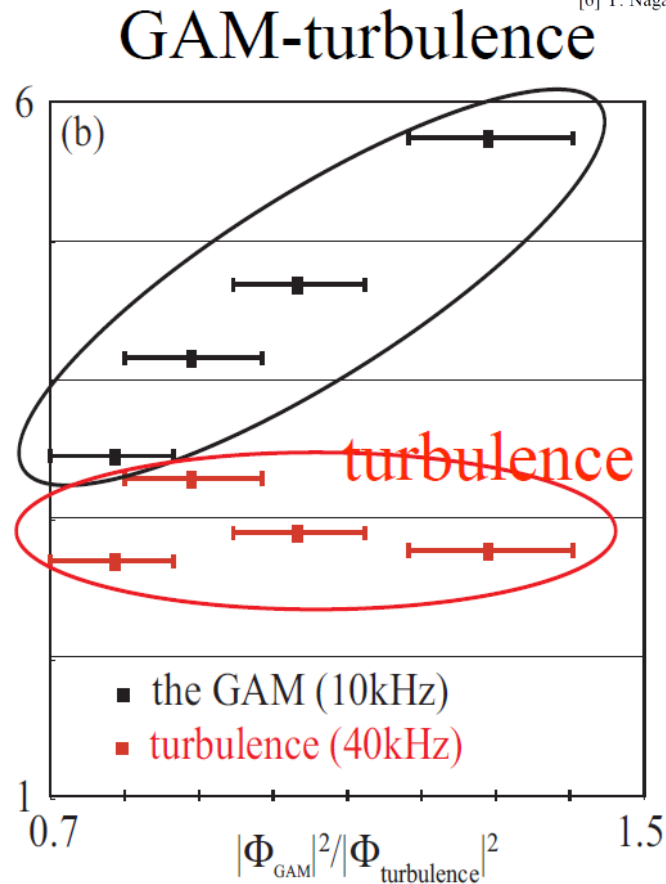
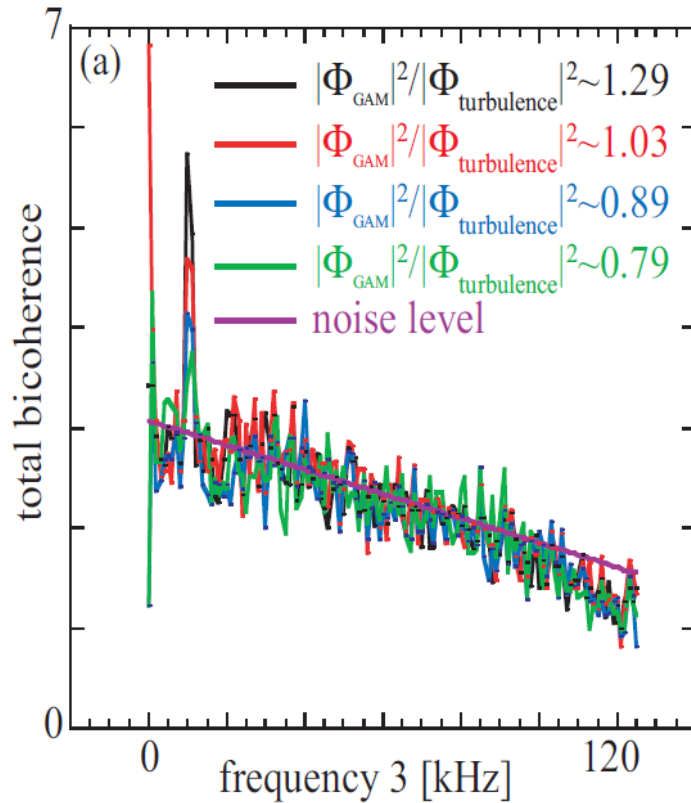
Total bicoherence at GAM is proportional to

$$|\phi_{\text{GAM}}|^2 / |\phi_{\text{drift}}|^2$$

[5] Y. Nagashima, et al., PRL 95, 095002 (2005),

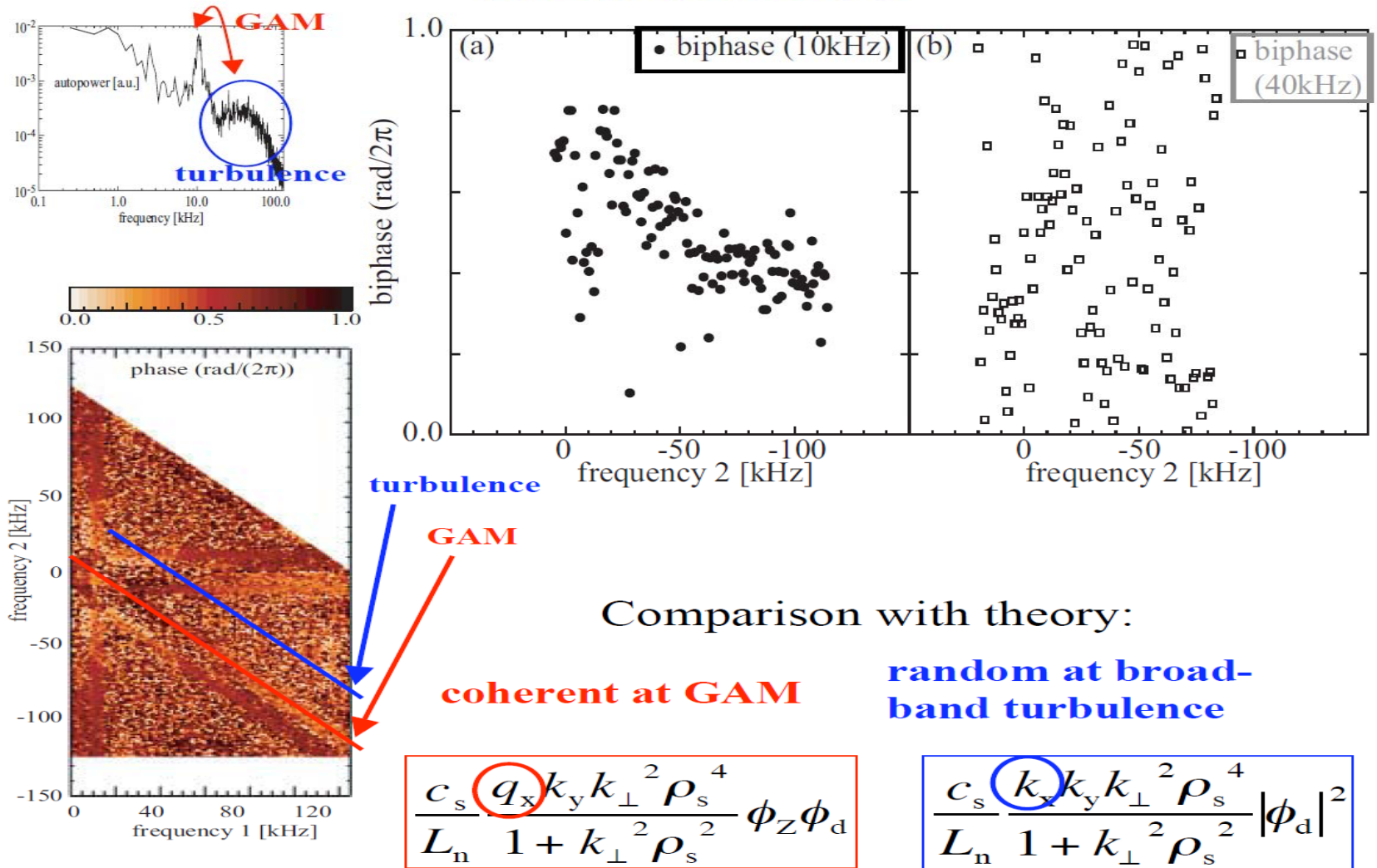
[6] Y. Nagashima, et al., PPCF 48, S1 (2006)

Experiments^[5]:



Biphase at GAM and broad-band turbulence

Experiments^[6]:

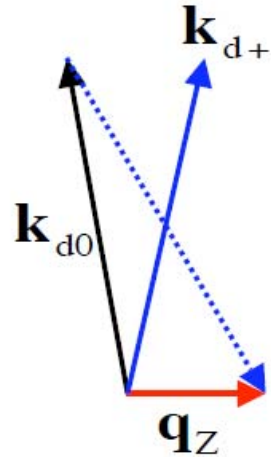


Biphases demonstrate the phase angles of nonlinear interaction terms in drift wave-zonal flow systems.

Proposal of GAM measurement by envelope modulation technique

Nonlinear property of the GAM

Four wave process(parametric-modulational instability)



$$\mathbf{k}_{d+} = \mathbf{k}_{d0} + \mathbf{q}_Z$$

$$\mathbf{k}_{d-} = \mathbf{q}_Z - \mathbf{k}_{d0}$$

Quoted from P.H. Diamond, et al.,
PPCF 47 R35 (2005)

k_{d0} : Primary drift wave wavenumber

k_{d+}, k_{d-} : Secondary drift wave wavenumbers

q_z : GAM radial wavenumber

Drift wave turbulence is modulated by zonal flows

---> **Envelope of the turbulence has ZF information.**

Drift waves have the condition $\frac{\tilde{\phi}}{T_e} \sim \frac{\tilde{n}}{n}$

--->**Close relationship between density and potential**

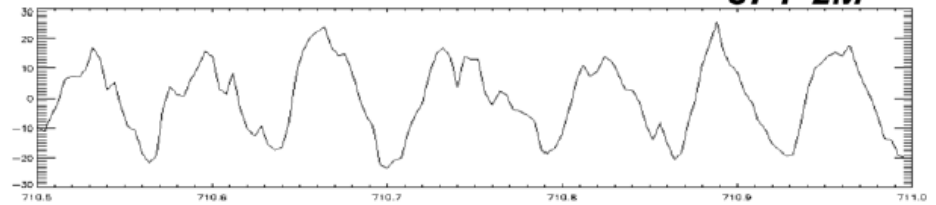
Envelope of turbulent density fluctuations has information of zonal flows

The envelop of the density fluctuation has the GAM info.

JFT-2M

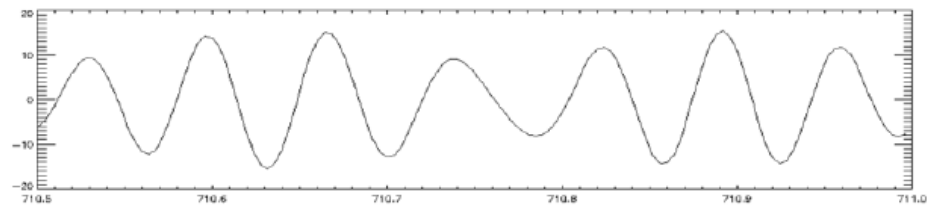
$\phi(t)$

Raw data



$\phi(t)$

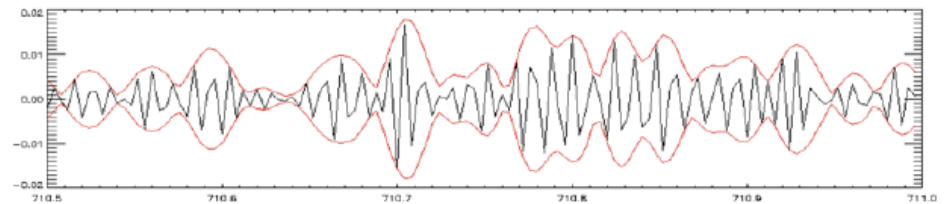
Band-pass (12 f 18 kHz, GAM frequency)



$n(t)$

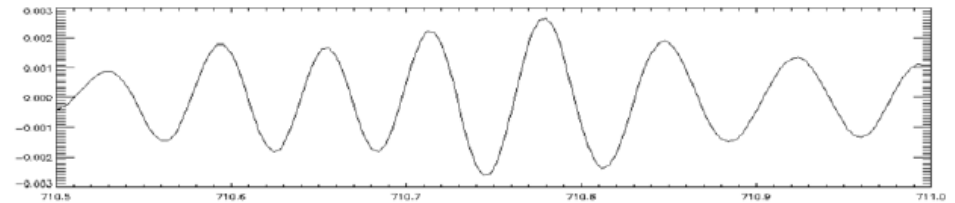
Black: high-pass (80 kHz f, frequency of turbulence)
Red: the envelope of black signals by Hilbert transform

$$Hf(\tau) = \int_{\mathbb{R}} \frac{f(t)}{t - \tau} dt$$



$n(t)$

Band-pass (12 f 18 kHz, GAM frequency)



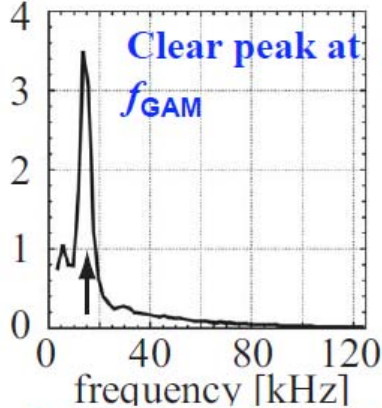
710.5

Time [msec]

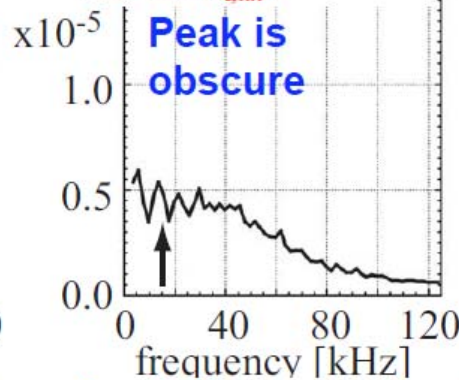
711

Quadratic spectra (Φ_f , $I_{i,sat}$, $Env(I_{i,sat})$)

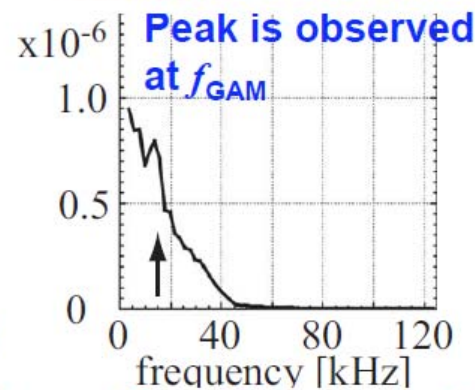
Floating potential (Φ_f)



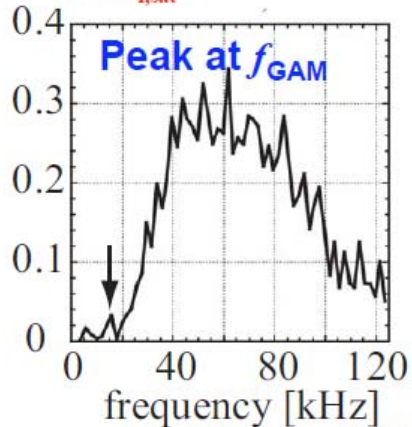
Ion saturation current ($I_{i,sat}$)



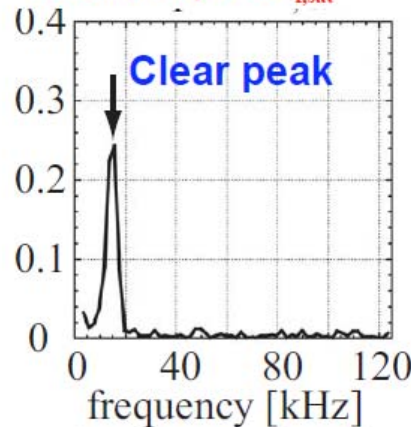
Envelope of ion saturation



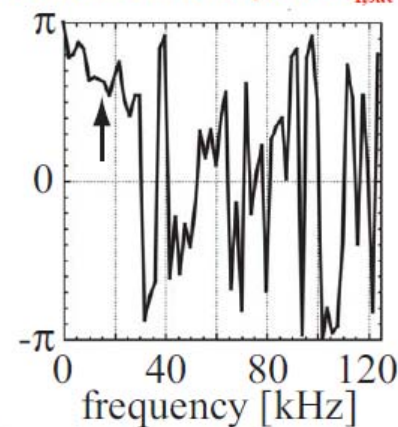
Correlation between Φ_f and $I_{i,sat}$



Correlation among Φ_f and the envelope of $I_{i,sat}$

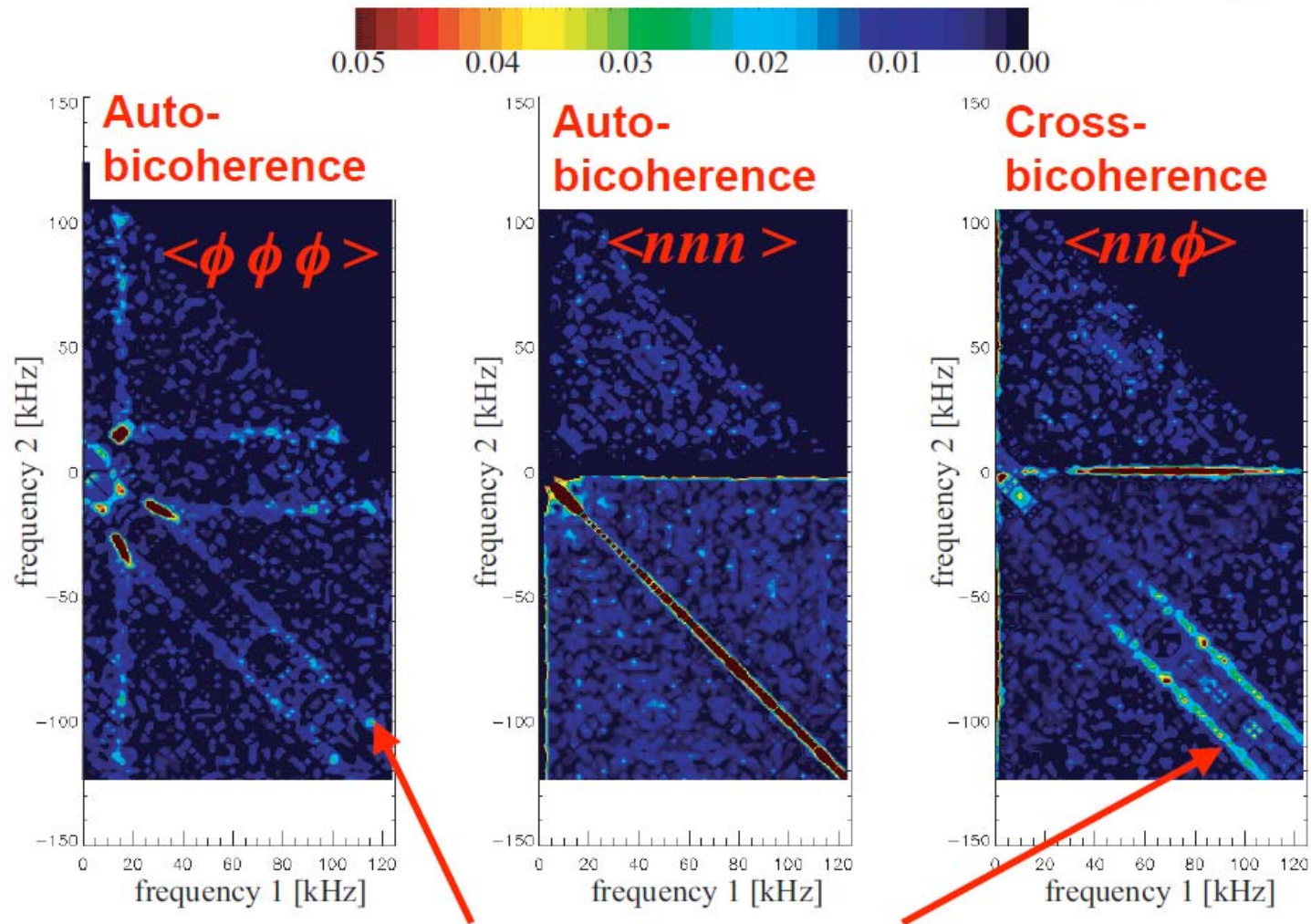


Cross phase among Φ_f and the envelope of $I_{i,sat}$



Significant correlation between Φ_f and the envelope of $I_{i,sat}$ at f_{GAM}

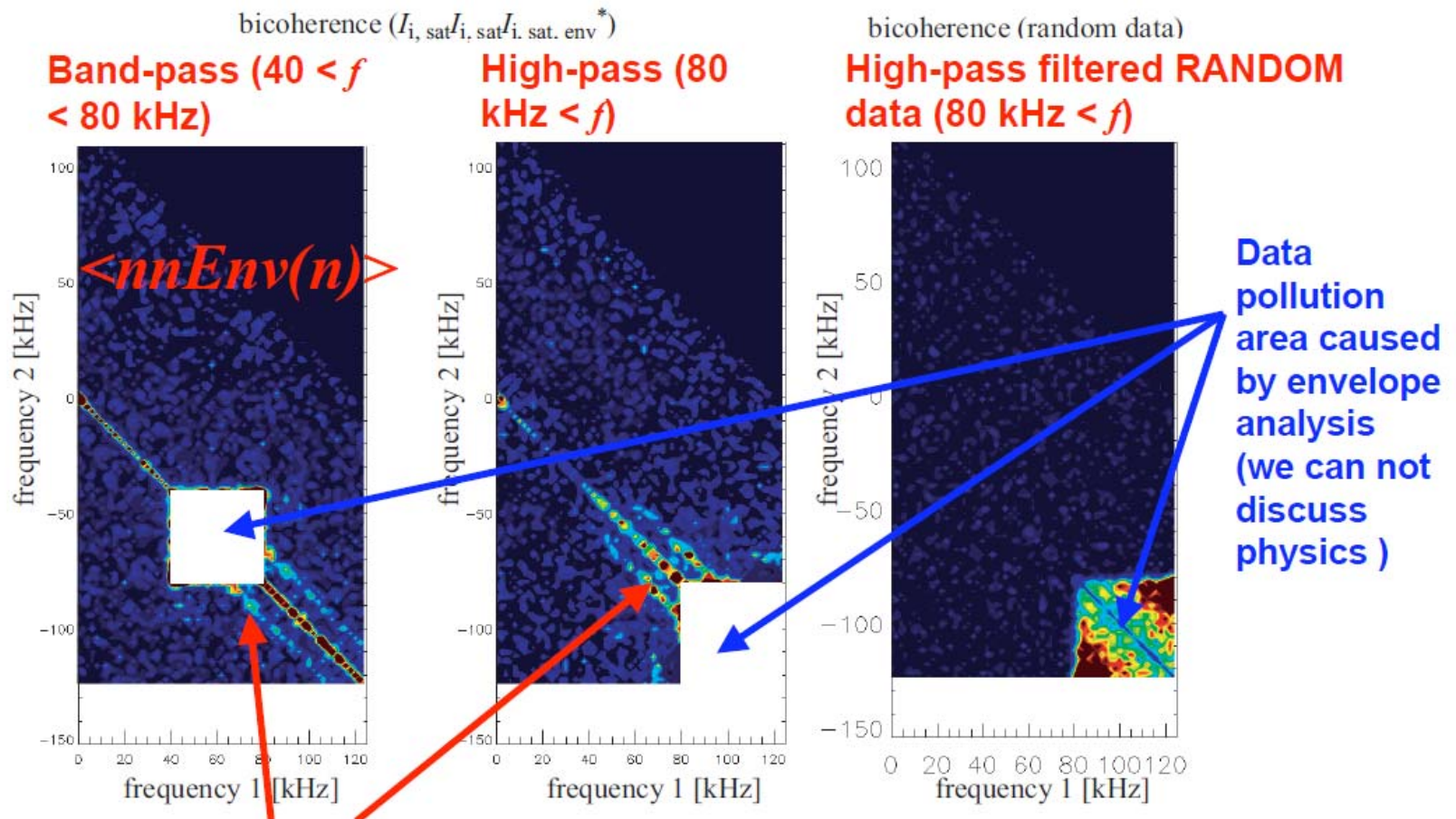
Auto/cross-bicoherence (Φ_f, I_{is})



Bicoherence between GAM and turbulence

Bicoherence of $nn\Phi_f$ is higher than that of $\Phi_f\Phi_f\Phi_f$

Cross-bicoherence (I_{is} , $Env(I_{is})$)



Significant bicoherence between the GAM and turbulence

Bicoherence between turbulence and the GAM is observed only by using density fluctuation data

**This research is applicable to
GAM spectroscopy (S.-I. Itoh,
et al. PPCF 49 L7 (2007))**

Bispectral analysis in linear plasmas

Analysis of momentum transfer

Energy transfer function T by use of $E_{r,ZV}$ [7]

$$\begin{aligned} T &= \sum_{k_{r,Z3}=k_{r,d1}+k_{r,d2}} k_{r,Z3} \operatorname{Im} \left\langle \tilde{u}_{r,d1} \tilde{u}_{\theta,d2} U_{\theta,Z3}^* \right\rangle \\ &= \sum_{k_{r,Z3}=k_{r,d1}+k_{r,d2}} k_{r,Z3} \operatorname{Im} \left\langle \frac{\tilde{E}_{\theta,d1} \tilde{E}_{r,d2}}{B^2} E_{r,Z3}^* \right\rangle \\ &\propto \sum_{k_{r,Z3}=k_{r,d1}+k_{r,d2}} k_{r,Z3} \operatorname{Im} \left\langle \tilde{E}_{\theta,d1} \tilde{E}_{r,d2} E_{r,Z3}^* \right\rangle \end{aligned}$$

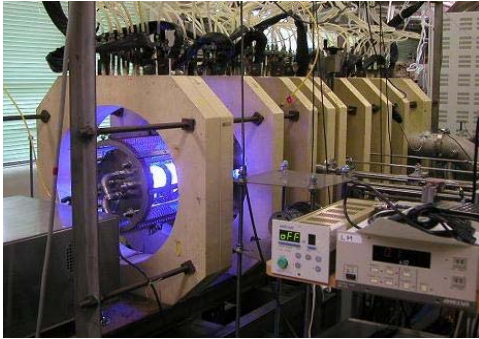
[7] G.R. Tynan, et al.,
Phys. Plasmas **8** (2001) 2691

**The analysis reflects local interaction of waves.
-->more precise analysis than potential analysis**

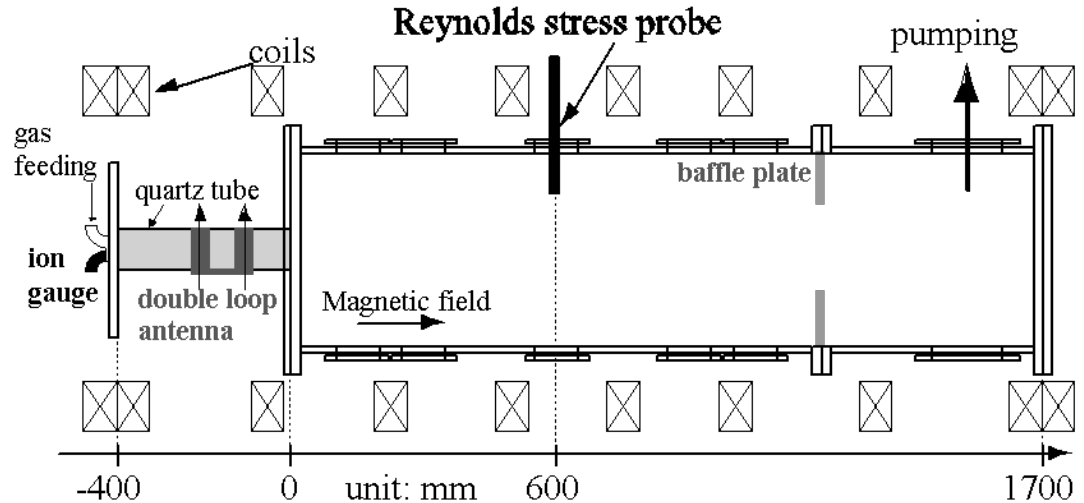
Experimental devices

The Large Mirror device (LMD [8])

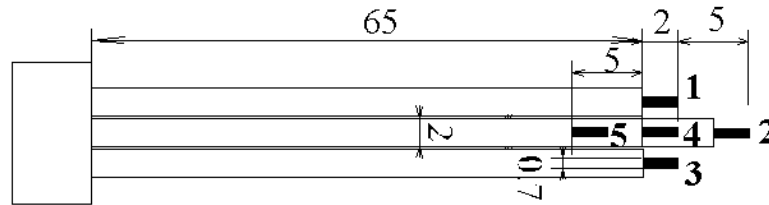
[8] Y. Saitou, et al., Phys. Plasmas **14** (2007) 072301



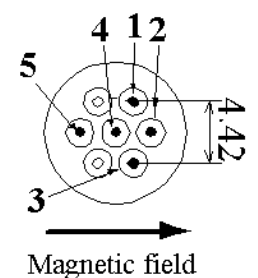
Helicon source (2kW, 7MHz) Ar gas



side view



top view



The Reynolds stress probe

$$\tilde{E}_\theta = (\tilde{\Phi}_1 - \tilde{\Phi}_3) / d_\theta \quad (k_\theta)$$

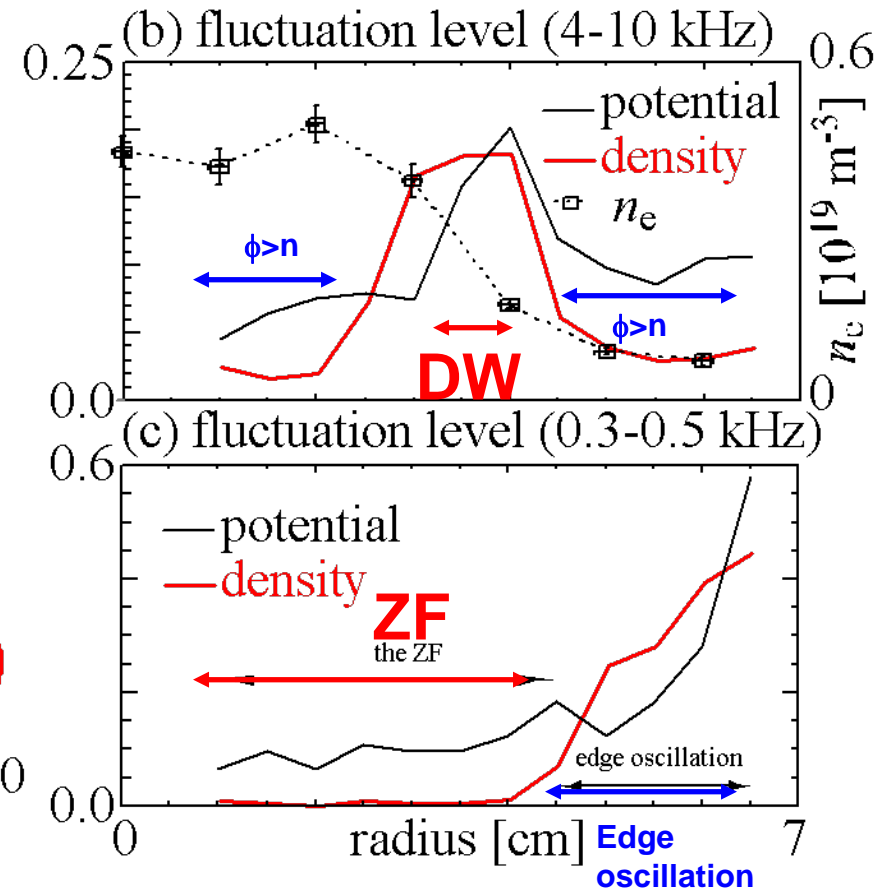
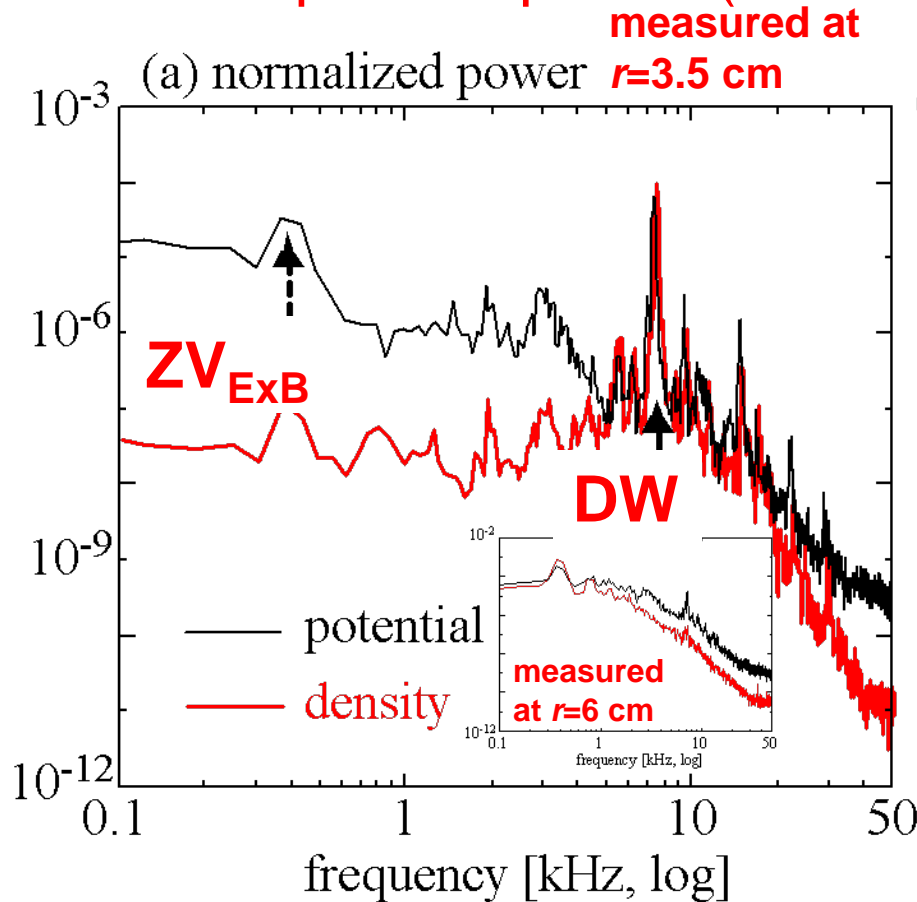
$$\tilde{E}_r = \{ \tilde{\Phi}_2 - (\tilde{\Phi}_1 + \tilde{\Phi}_3) / 2 \} / d_r \quad (k_r)$$

Reynolds stress per mass density $\langle \tilde{E}_r \tilde{E}_\theta \rangle / B^2$

Normalized fluctuation spectra

Normalized power spectra (at 0.3 sec)

Radial profiles

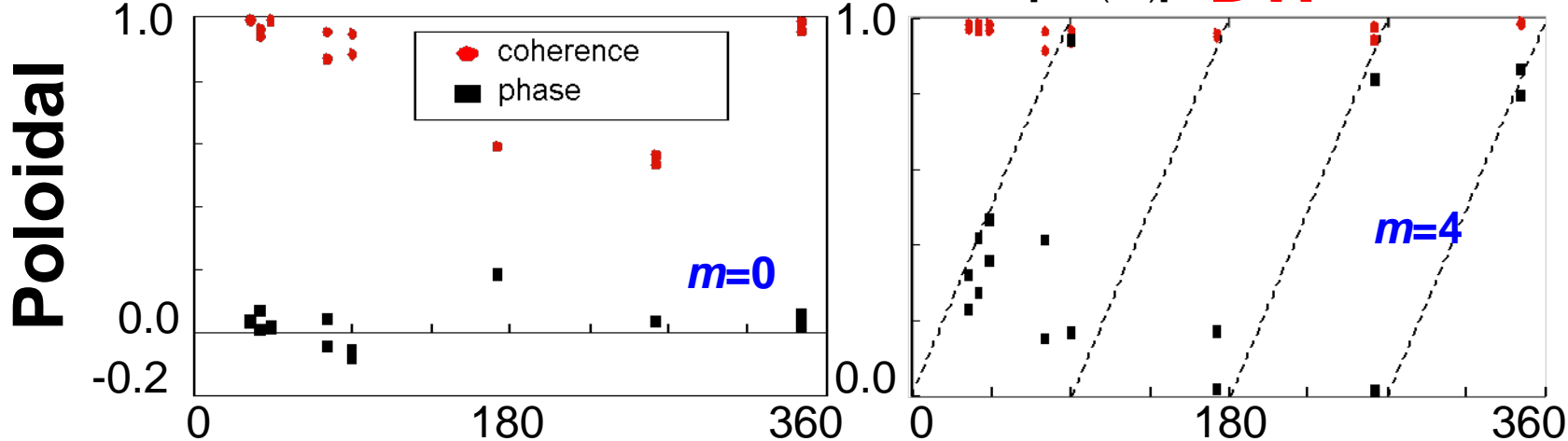


DW (density \sim potential) is located at $r=3.5-4$ cm.

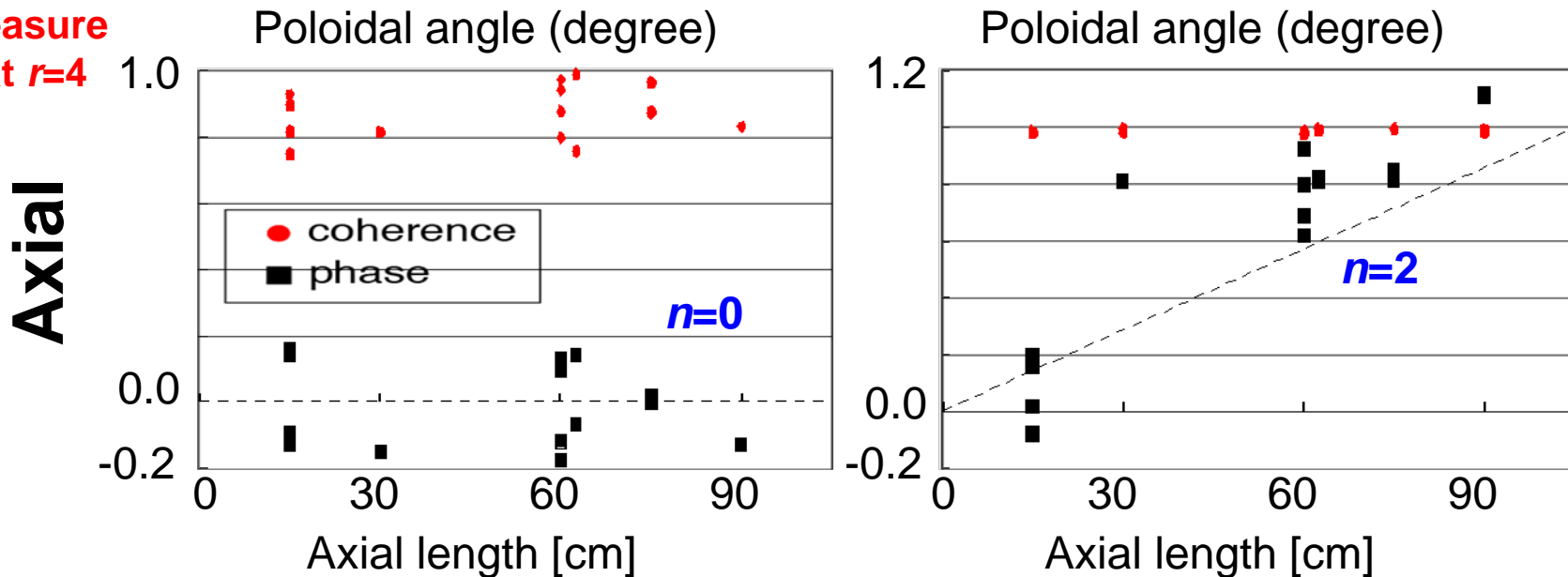
ZV_{ExB} exists at $r < \sim 4.5$ cm (edge oscillations $r > \sim 4.5$ cm).

Poloidal and axial wave numbers

Residual ZF coherence ■ phase [rad/(2π)] DW

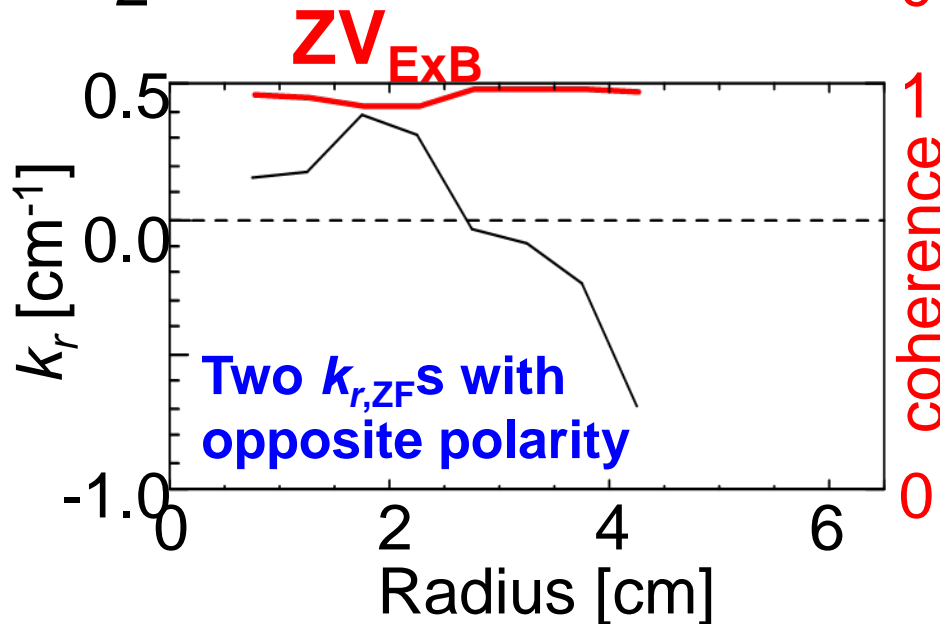
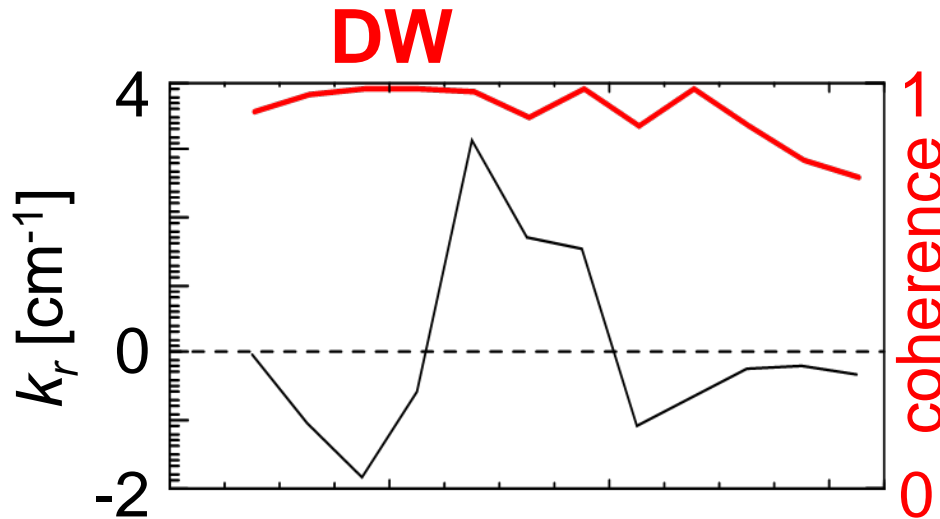


measure
d at $r=4$
cm

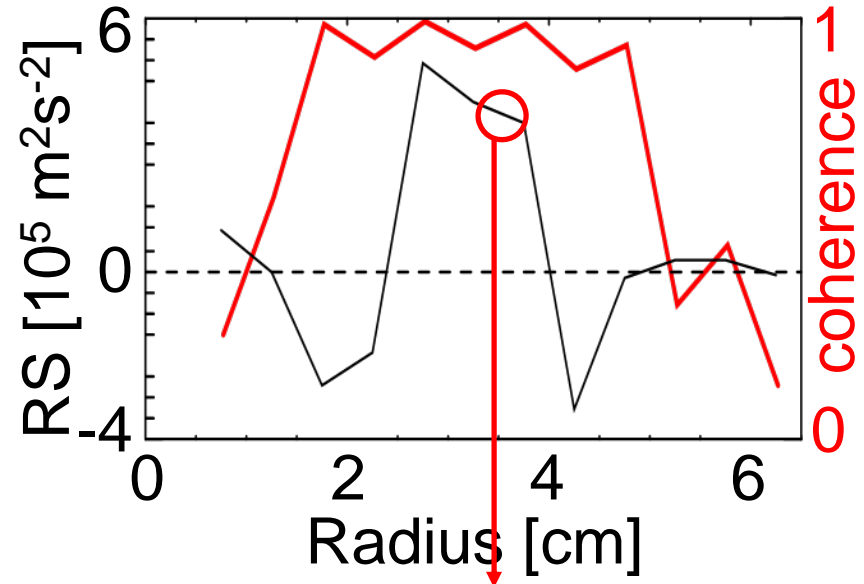


DW has $m=3-5$ and $n=2-3$, while residual ZF potential has $m, n \sim 0$.

Radial wave numbers (radial profile)



Time averaged Reynolds stress per mass density



$\omega_{de,th} = 6.22-8.26$ kHz at minimum RS gradient

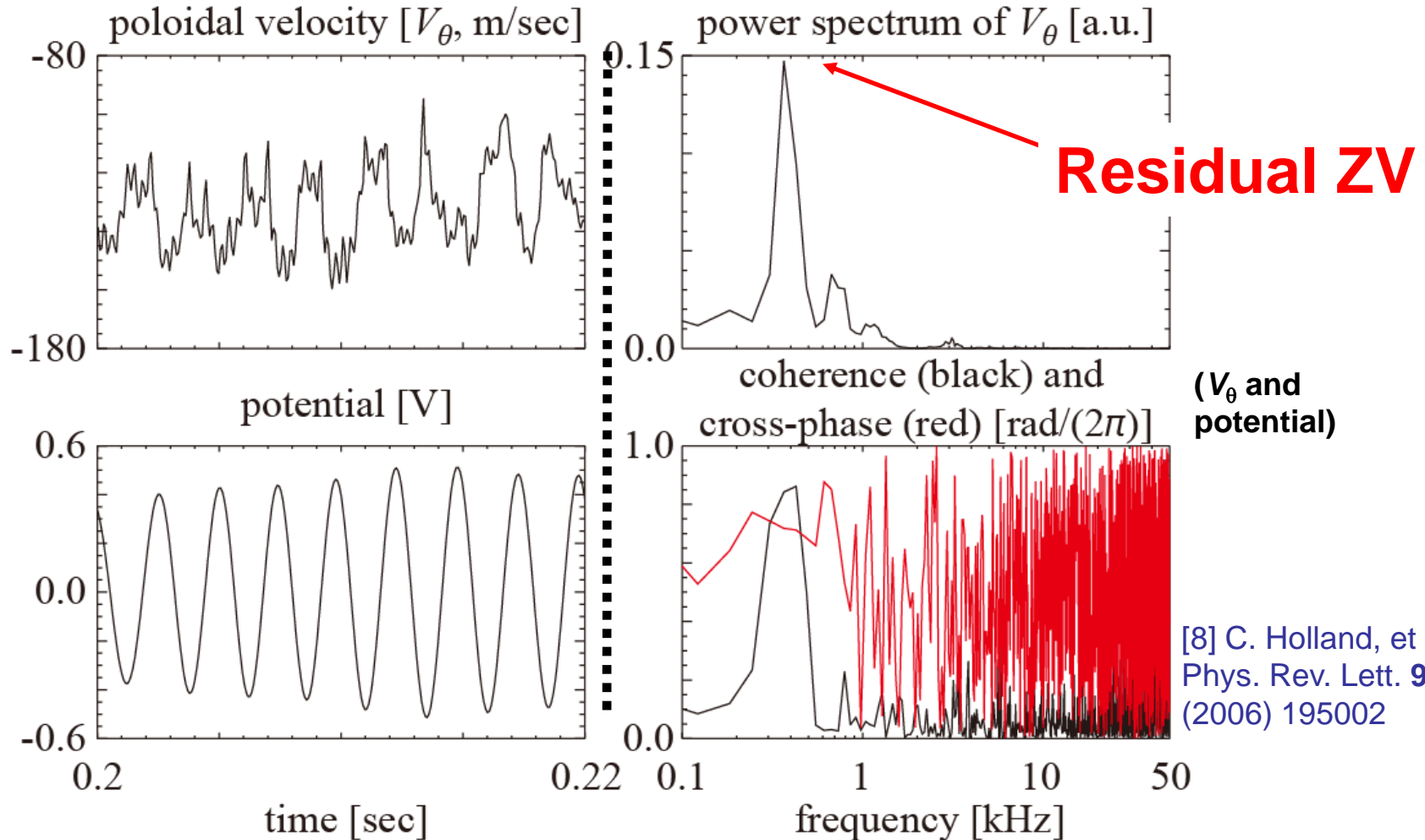
$\omega_{de,exp} = 7-8$ kHz

$$\omega_{de,th} = \frac{\omega_{*,e}}{1 + k_{\perp}^2 \rho_s^2}$$

ZV_{ExB} has two radial wave numbers with opposite polarity.

Poloidal velocity fluctuation

measured at $r=2.5$ cm where E_r of the ZV is large.

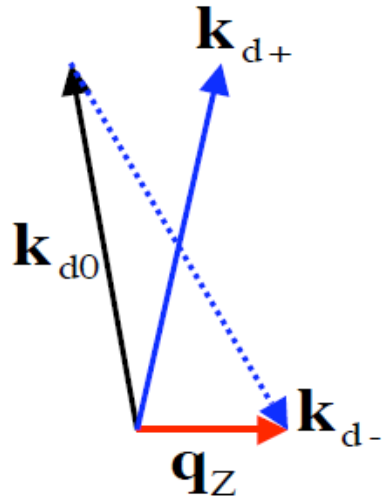


[8] C. Holland, et al.,
Phys. Rev. Lett. **96**
(2006) 195002

ZV is associated with the poloidal velocity fluctuation derived from the Time Delay Estimation^[8].

Y. Nagashima, et al.,
JPSJ 77 114501 (2008)

Four wave process(parametric-modulational instability)



$$\mathbf{k}_{d+} = \mathbf{k}_{d0} + \mathbf{q}_z$$

$$\mathbf{k}_{d-} = \mathbf{q}_z - \mathbf{k}_{d0}$$

Quoted from P.H. Diamond, et al.,
PPCF 47 R35 (2005)

k_{d0} : Primary drift wave wavenumber

k_{d+}, k_{d-} : Secondary drift wave wavenumbers

q_z : GAM radial wavenumber

Modulation of k , f , Φ_{zV} and $(v_r v_\theta)$

Notice: coordinate is corrected from left-handed (APS2007) to right-handed...

k_r, k_θ (two point cross-phase):

k_r modulation is significant.

k_θ or $V_{\theta,ph}$ is modulating at $r=4.25$ cm.

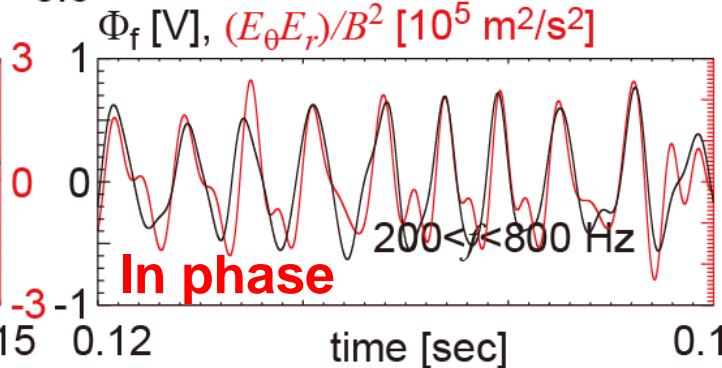
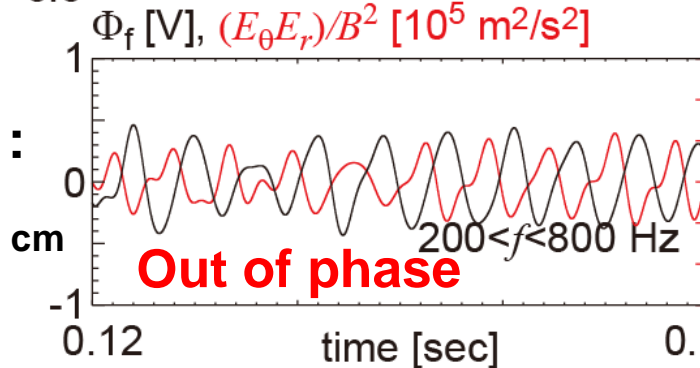
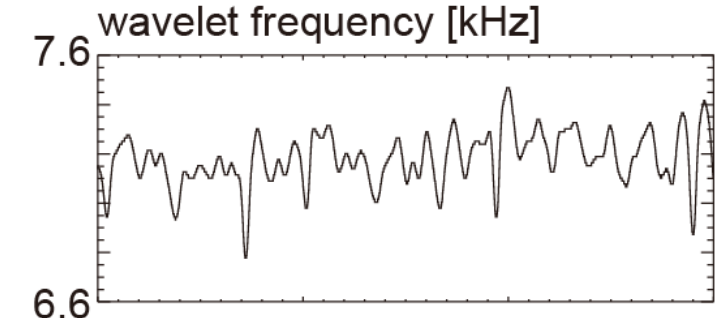
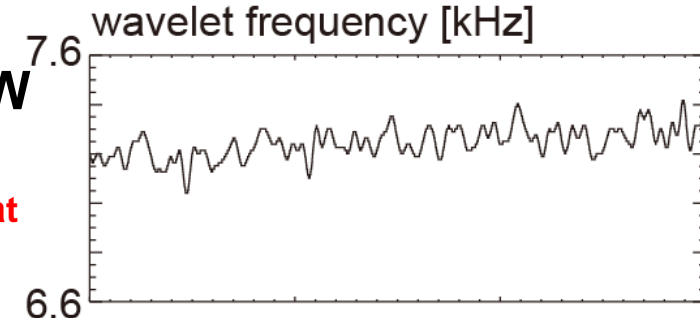
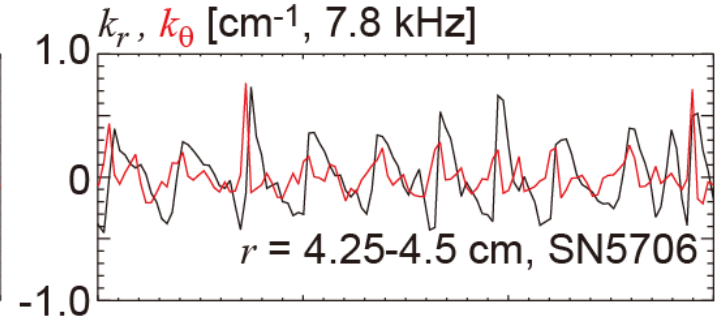
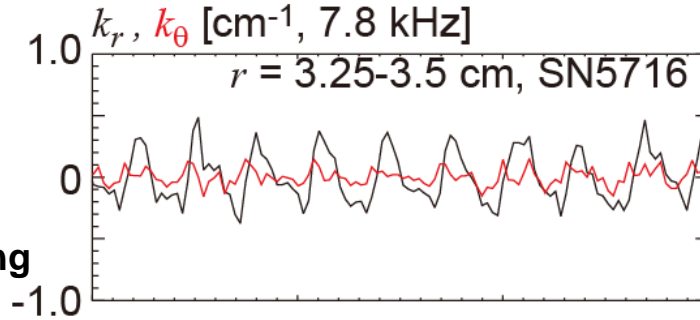
Peak f of the DW (wavelet):

f modulation is large at large $E_{r,zV}$ location.

$\Phi_{zV}, (E_\theta E_r)_{DW}/B$:

In phase at $r=4.25$ cm.

Out of phase at $r=3.25$ cm

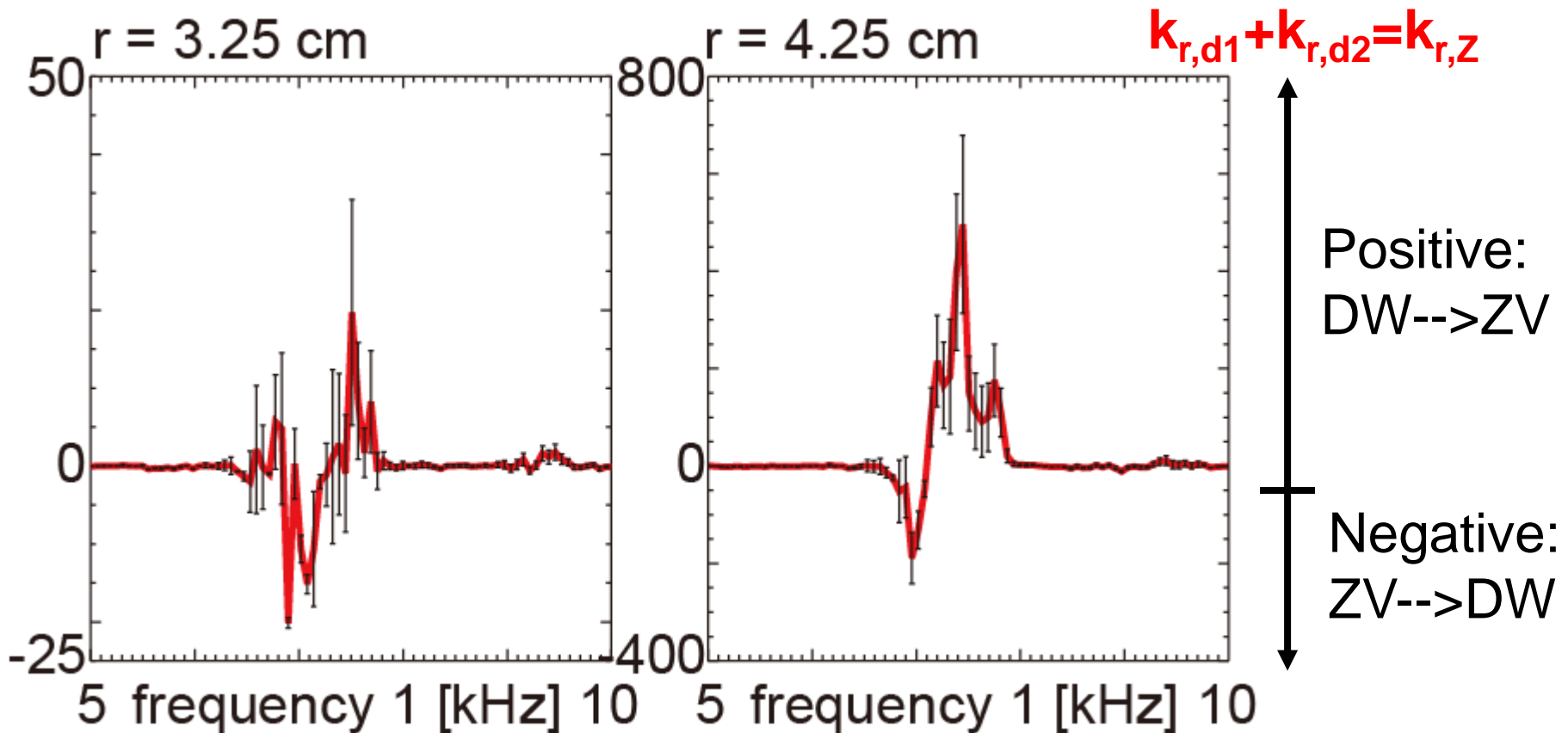


Measured at $r=3.25$ cm

Measured at $r=4.25$ cm

Modulational relationship is different in radius.

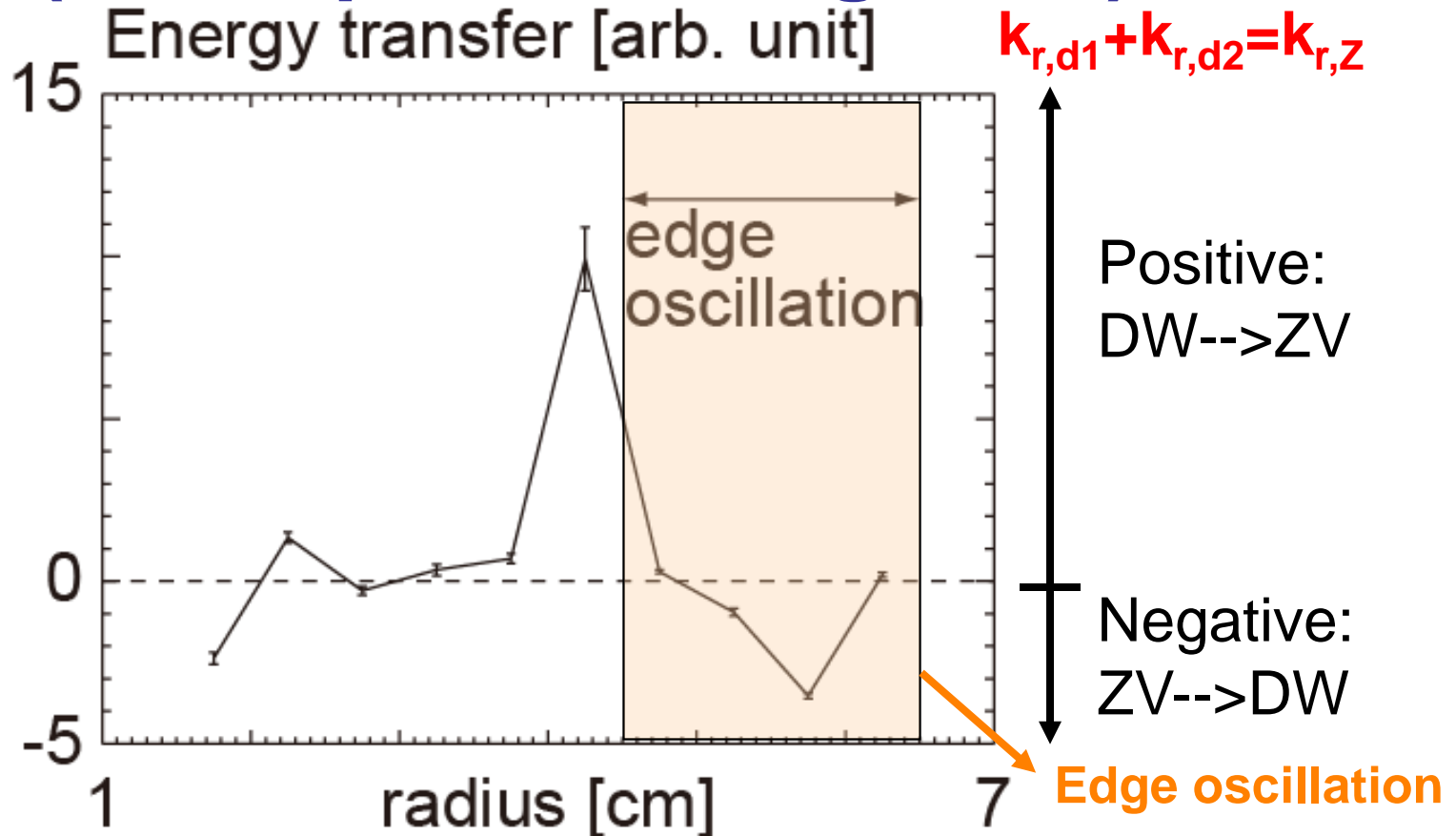
$(k_{r,d1} + k_{r,d2}) \text{Im}\langle E_{\theta,d} E_{r,d} E_{r,z}^* \rangle$
 estimation (frequency space)



Transfer direction is different in frequency.
 Momentum transfer from the DW to the ZV_{ExB}
 occurs totally at $r=4.25$ cm.

$$(k_{r,d1} + k_{r,d2}) \text{Im} \langle E_{\theta,d} E_{r,d} E_{r,z}^* \rangle$$

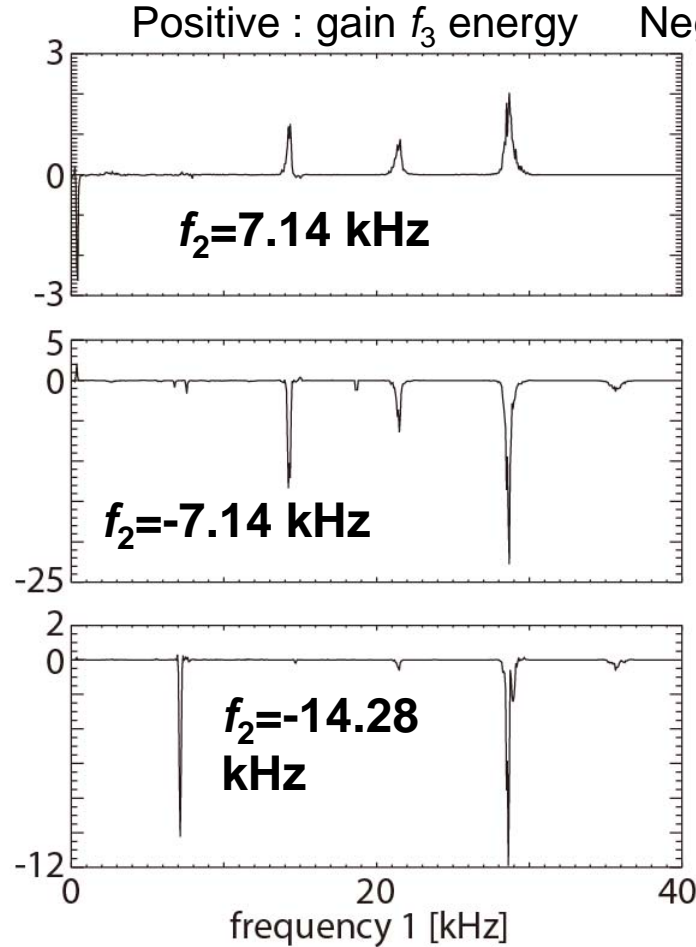
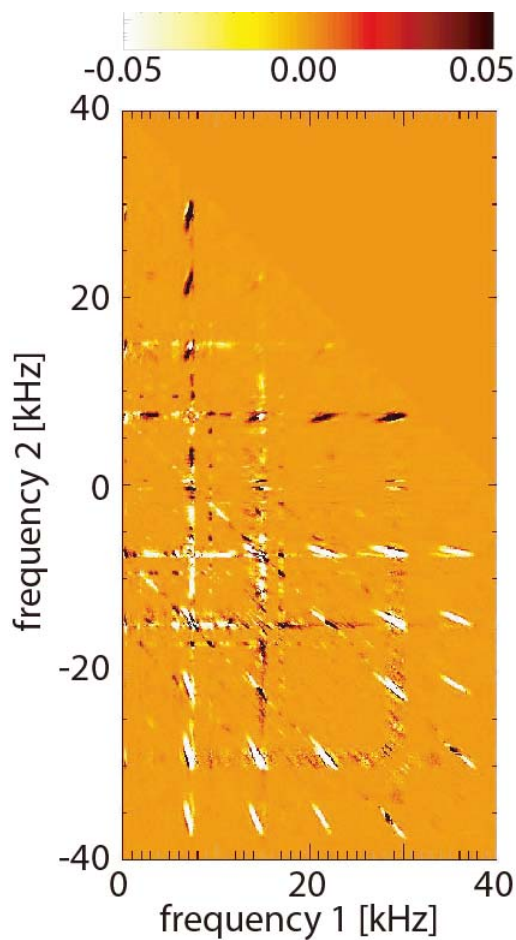
(radial profile, integrated)



Transfer direction is different in radius.

Strong momentum transfer from the DW to the ZV_{ExB} occurs at $r=4.25$ and 2.25 cm.

Estimation of Hasegawa-Mima type equation $\Sigma k_1 \times k_2 \cdot e_z \cdot (k_2^2 - k_1^2) \text{Re} \langle \Phi_1 \Phi_2 \Phi_3^* \rangle$



Positive : gain f_3 energy Negative : release f_3 energy

1: fundamental mode,
2: 2nd harmonic,...

1 + 2 --> 3,
1 + 3 --> 4,...

2 - 1 <-- 1,
4 - 1 <-- 3,...

4 - 2 <-- 2,...

r=3.25 cm

Forward transfer of the DW energy to higher harmonics occurs in frequency space

Conclusion

- 1. In the JFT-2M tokamak, bispectral analysis of the drift-wave-zonal flow turbulence succeeded in clarifying nonlinear process of turbulence.**
- 2. The combination of the bispectral and envelope analysis is proposed to detect GAMs by density fluctuation measurement and “GAM spectroscopy”.**
- 3. In the Large Mirror device (linear plasma device), coexistence of the low-frequency E_r oscillation and drift-wave fluctuation is observed.**
- 4. Nonlinear /nonlocal energy transfers between drift wave and the low-frequency E_r are identified in real and spectral spaces.**

Phase difference (Φ_f , and $Env(I_{is})$)

Theoretical prediction of phase shift between potential and the envelope

K. Itoh, et al., PPCF **47** (2005) 451

$$\frac{\delta|\phi_{\text{micro}}|^2}{|\phi_{\text{micro}}|^2} \cong \frac{4\rho_s^2 k_\theta^2}{\omega_{\text{GAM}}(1 + \rho_s^2 k_{\perp,0}^2)} \left(-i\theta s q_r^2 \phi \frac{B_z}{|B_z|^2} \right)$$

$$\propto -i\theta s q_r^2 \frac{B_z}{|B_z|}$$

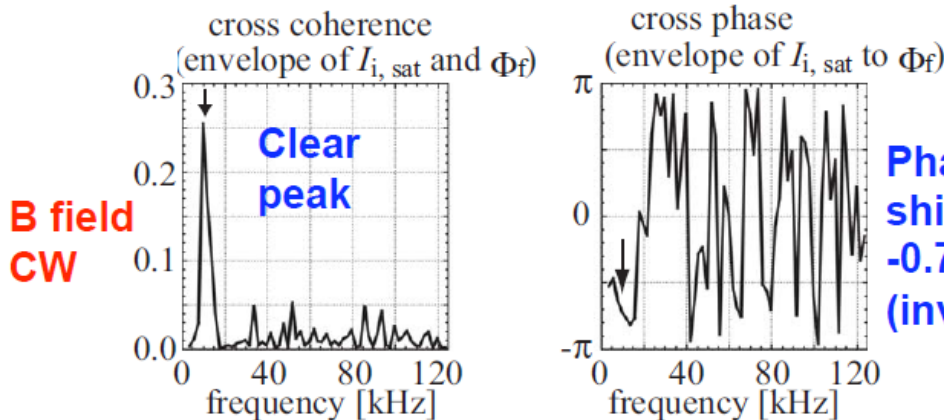
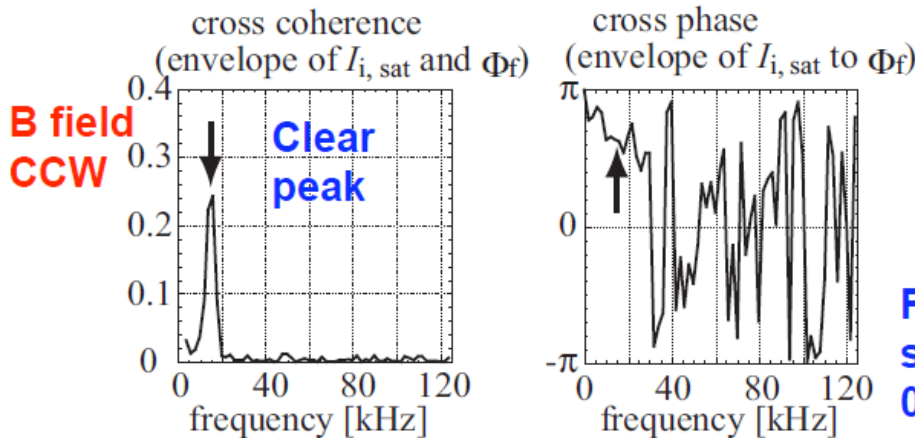
θ : poloidal angle
 s : shear parameter
 q_r : zonal flow radial wavenumber
 B_z : magnetic field

Phase shift
 $0.6 \sim 0.7\pi$

Phase shift
 $-0.7 \sim -0.8\pi$
 (invert)

Phase shift depends upon

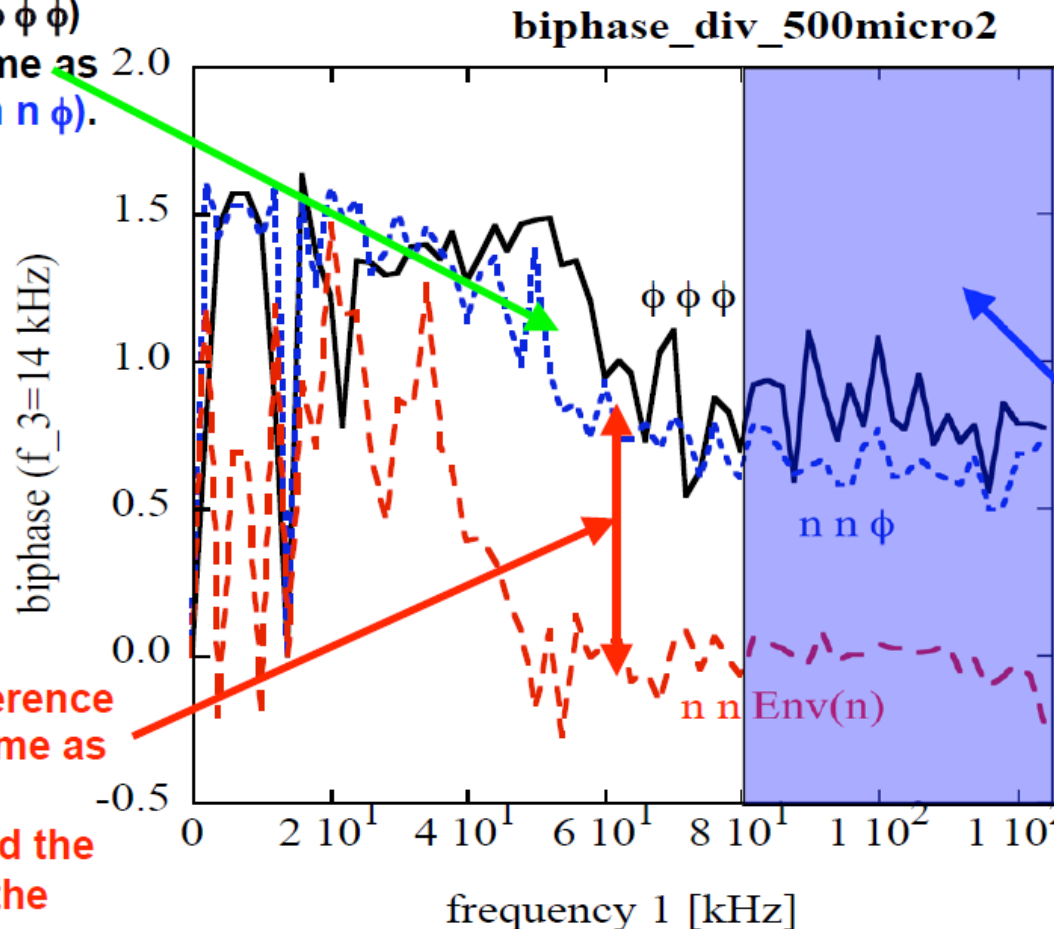
- Poloidal angle,
- shear parameter,
- complex radial wavenumber of zonal flow and
- direction of magnetic field



Inversion of phase shift is observed in opposite B direction

Biphase ($\Phi_f, I_{is}, Env(I_{is})$)

Biphase of ($\phi \phi \phi$) is almost same as biphase of ($n n \phi$).



High-pass filter $80 \text{ kHz} < f$ for envelope

Polluted area

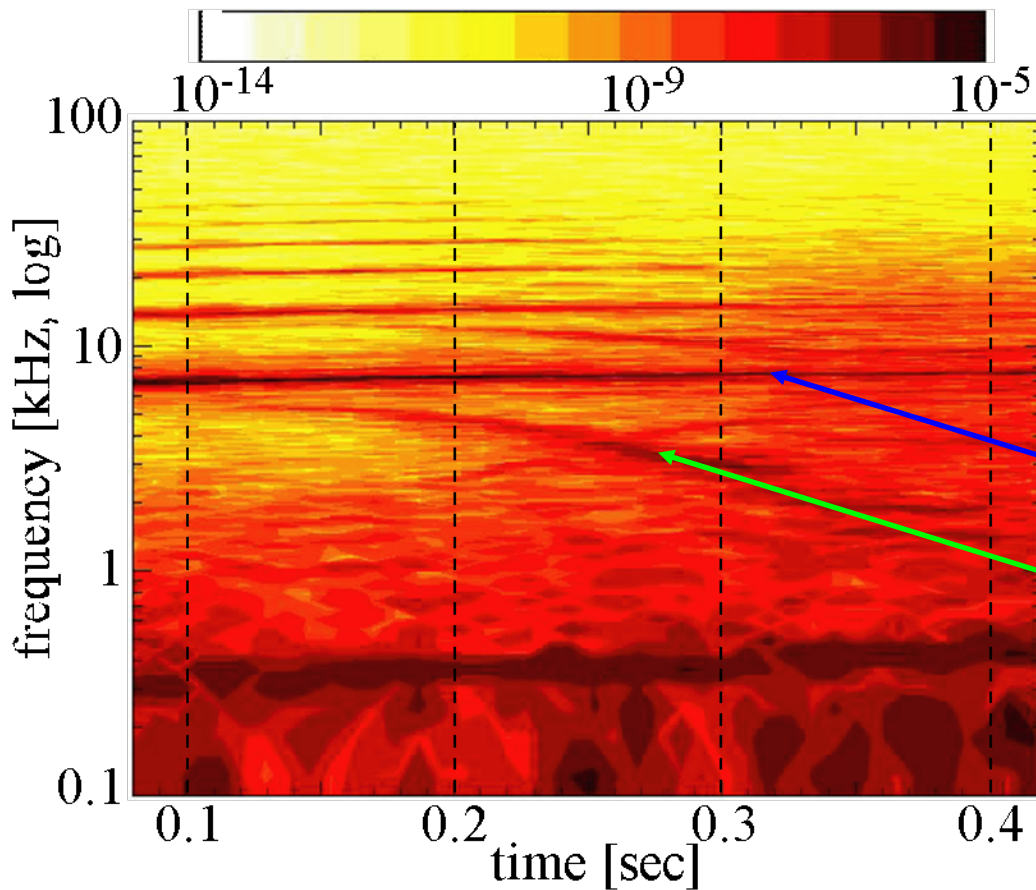
Biphase difference $\sim 0.7-0.8\pi$, same as phase shift between f and the envelope of the GAM

Biphase analysis is applicable

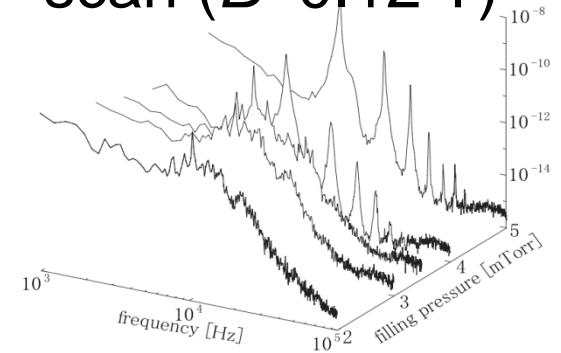
considering phase between ϕ and the envelope

The drift wave and the zonal ExB flow

Time evolution of the potential spectrum during a single discharge



Filling pressure scan ($B=0.12$ T)



Marginal transition to strong turbulence at 3.5 mTorr

the Drift Wave (DW)

quasi-modes
(future scope)

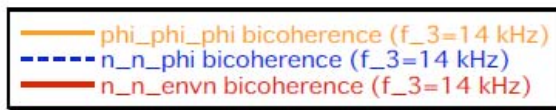
the residual Zonal
ExB Velocity (ZV_{ExB})

Measured at $r=3.5$ cm (plasma radius $a \sim 5$ cm)

DW (7-8 kHz) and residual ZV_{ExB} (~ 400 Hz) are observed.

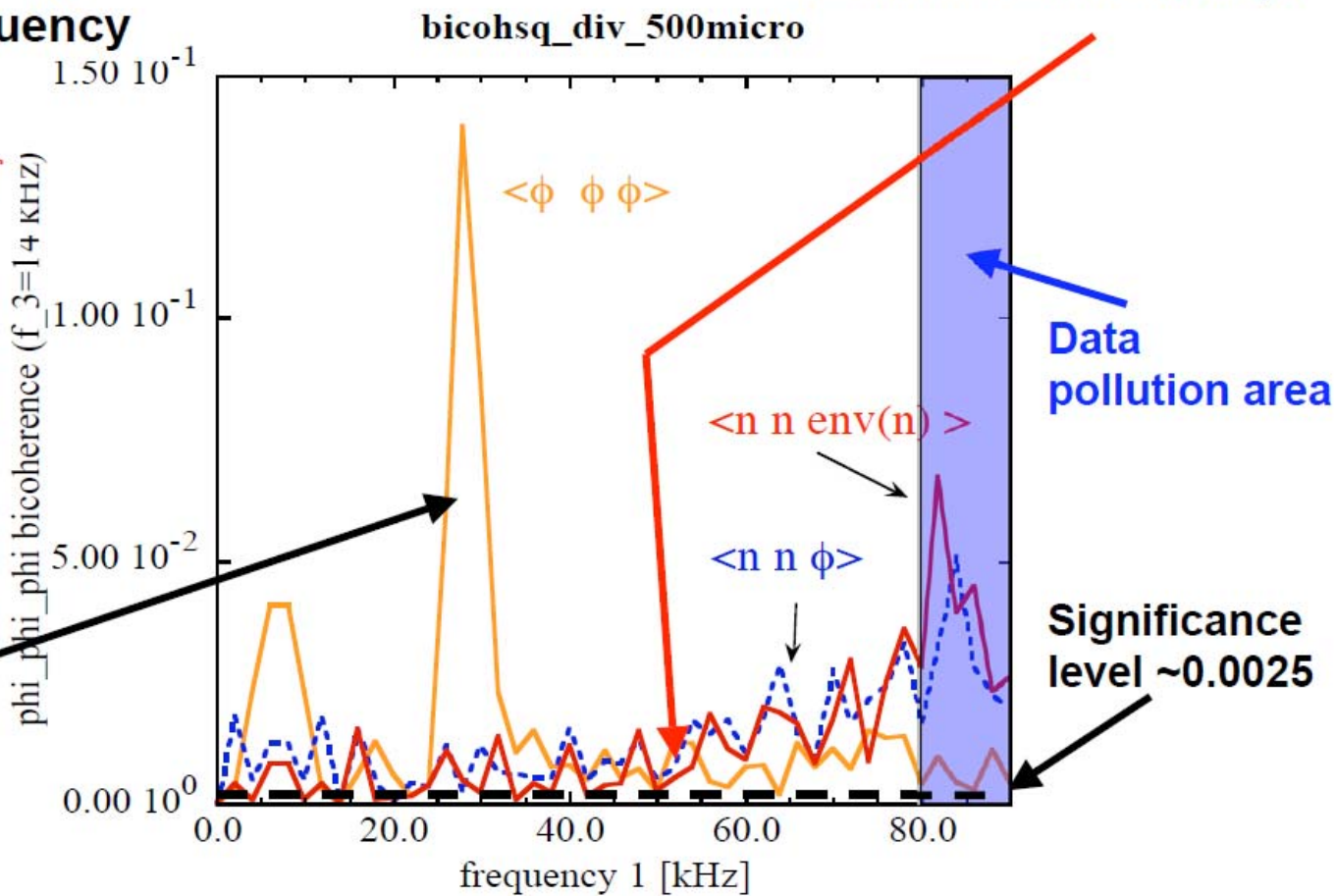
Comparison of bicoherence

Cross-section of bicoherence at $f_3 =$ the GAM frequency



Bicoherence of $(n n env(n))$ is similar to that of $(n n \phi)$

High-pass filter 80 kHz $< f$ for envelope



Self coupling of GAM in $(\phi \phi \phi)$, which is not observed in $(n n \phi)$

Bicoherence of $\langle nnEnv(n) \rangle$ is same as that of $\langle nn\Phi \rangle$